

Heterogeneous Integration of GaInAsSb p-i-n Photodiodes on a Silicon-on-Insulator Waveguide Circuit

Nannicha Hattasan, Alban Gassenq, Laurent Cerutti, Jean-Baptiste Rodriguez, Eric Tournié, and Gunther Roelkens

Abstract—We report the integration of GaInAsSb p-i-n photodiodes on a silicon-on-insulator waveguide circuit. The device operates with low dark current ($1.13 \mu\text{A}$ at -0.1 V) at room temperature. A high responsivity of 0.44 A/W is measured at $2.29 \mu\text{m}$. This yields $1.63 \times 10^9 \text{ cmHz}^{1/2}/\text{W}$ of Johnson-noise-limited-detectivity.

Index Terms—GaInAsSb, heterogeneous integration, photodiode.

I. INTRODUCTION

SEVERAL bio-molecules and gases such as glucose, CH_4 , CO_2 and CO have strong overtone and combination absorption lines in the near and mid-infrared, particularly in the 2 to $2.5 \mu\text{m}$ wavelength range. In this wavelength region, absorption spectroscopy can be used to analyze the composition of an analyte through the absorption signatures of the molecules. A number of sources and detectors have been proposed over the past few years for this goal [1]–[3]. However, these are discrete opto-electronic components. Integration of such components on a waveguide platform would open a whole new range of applications for mid-wave infrared systems. Silicon photonics has advantages in terms of cost and complementary metal-oxide-semiconductor (CMOS) compatible fabrication for photonic integrated circuits in the telecommunication wavelength range [4], [5]. Given its transparency from 1.2 to $3.5 \mu\text{m}$, it is possible to realize integrated spectroscopic systems on this platform by combining active opto-electronic devices on silicon-on-insulator (SOI) passive waveguide circuits. Several works have been reported towards this goal, for example, the integration of

Manuscript received June 27, 2011; revised September 12, 2011; accepted September 14, 2011. Date of publication September 22, 2011; date of current version November 04, 2011. This work was supported in part by the Glucosens project Grant IWT-SBO and by the Miracle project.

N. Hattasan is with the Photonics Research Group, INTEC-Department, Ghent University-IMEC and Center for Nano- and Biophotonics (NB-Photonics), Ghent 9000, Belgium (email: nannicha.hattasan@intec.ugent.be).

A. Gassenq and G. Roelkens are with the Photonics Research Group, INTEC-Department, Ghent University-IMEC and Center for Nano- and Biophotonics (NB-Photonics), Ghent 9000, Belgium (e-mail: agassenq@intec.ugent.be; gunther.roelkens@intec.ugent.be).

L. Cerutti, J.-B. Rodriguez, and E. Tournié are with the IES – CNRS UMR5214, University Montpellier 2, 34095 Montpellier, France (e-mail: cerutti@univ-montp2.fr; rodriguez@ies.univ-montp2.fr; etournie@univ-montp2.fr).

Color versions of one or more of the figures in this letter are available online at <http://ieeexplore.ieee.org>.

Digital Object Identifier 10.1109/LPT.2011.2169244

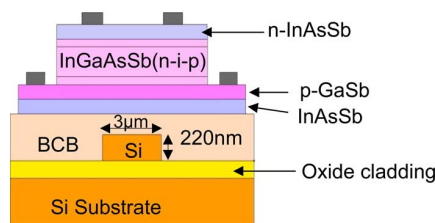


Fig. 1. Cross-section schematic of the device.

metal-semiconductor-metal and Ge photodetectors, using different integration techniques [6], [7]. The realizations so far are however focused on telecommunication applications in the $1.55 \mu\text{m}$ wavelength range.

In this letter we present the first heterogeneous integration of GaInAsSb p-i-n photodiodes (grown lattice matched on a GaSb substrate) on SOI waveguide circuits.

Our integration approach is based on adhesive bonding using the Benzocyclobutene (DVS-BCB) as an adhesive bonding agent.

A dark current of $1.13 \mu\text{A}$ at -0.1 V corresponding to a current density of 186 mA/cm^2 and a responsivity of 0.44 A/W at $2.29 \mu\text{m}$ are obtained, resulting in a $\sim 24\%$ external quantum efficiency. The device operates at room temperature.

II. DESIGN AND SIMULATION

The device schematic is shown in Fig. 1. It consists of a $3 \mu\text{m}$ wide by 220 nm thick silicon-on-insulator waveguide onto which a GaInAsSb epitaxial layer stack is bonded using DVS-BCB adhesive bonding. Light is coupled from the SOI waveguide into the photodetector using evanescent coupling. Optimal coupling can be achieved by controlling the phase matching between the SOI waveguide and the photodiode waveguide. The simulation of the coupling efficiency as a function of the photodetector thickness is carried out using Cavity Modelling Framework (CAMFR), a full-vectorial 2-D eigenmode expansion method. The simulation result is shown in Fig. 2 for a $20 \mu\text{m}$ long device. It shows that the maximum absorption is achieved when the thickness of the photodiode is such that the waveguide mode phase matches with the Si waveguide mode.

The epitaxial stack consists of 50 nm p-doped ($1.0 \times 10^{18} \text{ cm}^{-3}$) GaSb and a 50 nm p-doped ($1.0 \times 10^{18} \text{ cm}^{-3}$) $\text{Ga}_{0.79}\text{In}_{0.21}\text{As}_{0.19}\text{Sb}_{0.81}$ layer as the p-zone of a p-i-n layer stack. A not intentionally doped 500 nm thick $\text{Ga}_{0.79}\text{In}_{0.21}\text{As}_{0.19}\text{Sb}_{0.81}$ layer is used for the intrinsic absorbing region which is indicated as the optimum

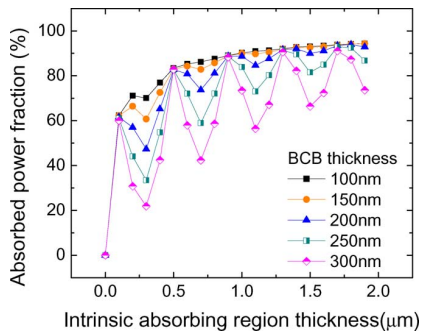


Fig. 2. Simulation showing the impact of absorbing region thickness and DVS-BCB thickness on detection efficiency.

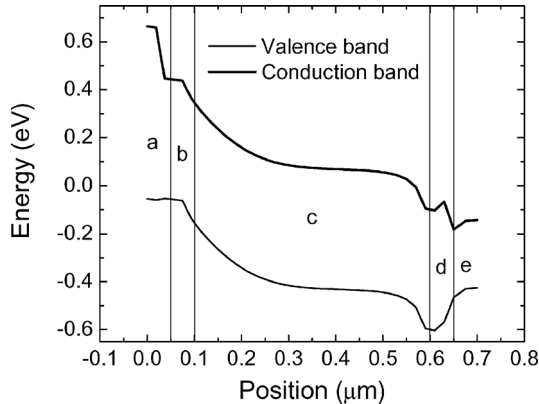


Fig. 3. Energy band diagram of the integrated photodetector indicating region (a) as GaSb p-doped, (b), (c), and (d) as p-i-n GaInAsSb, respectively, and (e) as InAsSb n-doped.

point from the simulation. The n-type region consists of 50 nm $\text{Ga}_{0.79}\text{In}_{0.21}\text{As}_{0.19}\text{Sb}_{0.81}$ and 50 nm $\text{InAs}_{0.91}\text{Sb}_{0.09}$. Both are doped to $1.0 \times 10^{18} \text{ cm}^{-3}$. An $\text{InAs}_{0.91}\text{Sb}_{0.09}$ layer is chosen as n-contact because of its lower bandgap (0.35 eV) and low contact resistance [8], [9].

The energy band diagram is presented in Fig. 3. The diffusion of minority carriers is prevented on the p-type side by the use of a wide bandgap GaSb layer. The cut off wavelength of this epitaxial stack is estimated to be $2.5 \mu\text{m}$.

III. DEVICE FABRICATION

The fabrication process can be divided into 3 parts: SOI waveguide fabrication, epitaxial growth, and photodiode fabrication. SOI waveguides are processed with standard CMOS technology. 193 nm deep UV lithography is used for pattern definition and the waveguides are dry etched [10].

The epitaxial stack is grown by Molecular beam epitaxy (MBE) on a n-type GaSb substrate [11]. Adhesive bonding is used for the integration of the epitaxial layers onto the SOI chip [12]. DVS-BCB is applied on the SOI chip by spin coating. The epitaxial layer stack is then attached upside down onto the SOI waveguide circuit. The DVS-BCB is then cured at 250°C for 1 hr. The bonding thickness can be varied by diluting the DVS-BCB solution with varying volumes of mesitylene. Successful bonding of the GaSb-based epitaxy with 68 nm of DVS-BCB was demonstrated. After the bonding process, the GaSb substrate is removed by wet etching with a mixture of HF, CrO_3 and water (1:1:3 v/v) at room temperature, using the InAsSb layer as an etch stop layer. InAsSb is removed

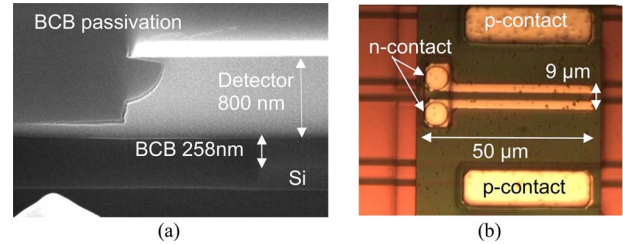


Fig. 4. (a) Cross-section SEM image. (b) Optical image of the device.

before n-contact deposition by using a mixture of citric acid and hydrogen peroxide (100:50 v/v). The mesa is formed by a combination of both dry ($\text{CH}_4:\text{H}_2$) and wet etching (citric acid: $\text{H}_2\text{O}_2:\text{H}_3\text{PO}_4:\text{H}_2\text{O}$ 55:5:3:220 v/v) to reduce the dark current. Ti(2 nm)/Pt(35 nm) and Au(100 nm) is deposited using e-beam evaporation for both contacts. DVS-BCB (1.3 μm thick) is then spin-coated on the sample and cured at 250°C for 1 h to passivate the device. Fig. 4(a) is a SEM cross section image of the fabricated photodetector, showing undercut due to the wet etching process. The bonding thickness for the reported devices is 258 nm. The original process scheme included the removal of the InAsSb cap layer to obtain a clean surface before bonding. However, this created a hydrophilic surface which prevented good bonding with DVS-BCB. Therefore, the InAsSb cap layer was kept in this experiment. The mesa is 9 μm wide and 50 μm long (Fig. 4(b)).

IV. MEASUREMENT RESULTS

The experimental setup consists of a continuous wave short-wave-infrared tunable laser which is coupled to a single mode fiber. After polarization control, TE-polarized light from a single mode fiber is injected into the SOI waveguide through a grating coupler structure defined in the silicon waveguide layer. The gratings have approximately -9 dB peak coupling efficiency at $2.27 \mu\text{m}$ with a 200 nm 3 dB-bandwidth. The distance between the grating coupler and the device is 400 μm . Therefore, the loss due to the propagation in the waveguide can be neglected. The reference signal before injecting into the chip is measured from single mode fiber using an optical spectrum analyzer (AQ6375 from Yokogawa).

The photoresponse measured at $2.25 \mu\text{m}$ at different fiber input power levels is shown in Fig. 5. Good linearity is obtained over a 12 dB input power range in Fig. 5. Due to the space charge induced electric field, an increase of reverse bias voltage is required to extract all generated carriers when the input power increases. The dark current at -0.1 V is $1.13 \mu\text{A}$ at room temperature. This corresponds to a current density of $186 \text{ mA}/\text{cm}^2$. We performed initial investigations on R_0A versus perimeter-to-area ratio of the photodiode; we obtain an R_0A ranging from 1.6 (for a $180 \mu\text{m}$ by $180 \mu\text{m}$ device) to $0.53 \Omega \cdot \text{cm}^2$ (for a $60 \mu\text{m}$ by $60 \mu\text{m}$ device). It shows a strong dependence on perimeter-to-area which suggests that side wall leakage is a limiting factor. This can be improved by changing the mesa etching condition, for example, by wet etching and using a passivation process such as applying ammonia sulfide before DVS-BCB passivation.

In this experiment, we obtain a peak fiber to detector responsivity of $0.06 \text{ A}/\text{W}$ at $2.29 \mu\text{m}$. Based on our initial measure-

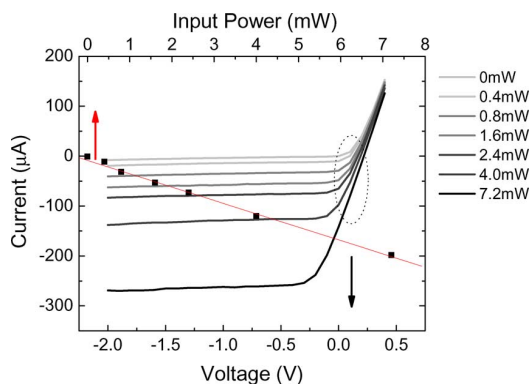


Fig. 5. V - I characteristics at different fiber input power levels measured at $2.25\text{-}\mu\text{m}$ wavelength. (■) Photocurrent measured at -0.1 V with different input power levels showing good linearity.

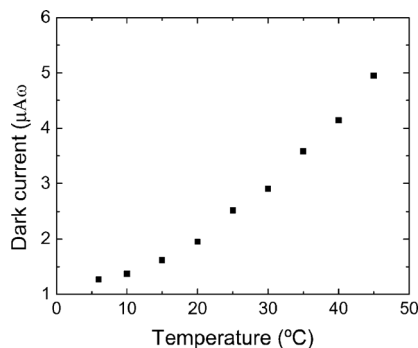


Fig. 6. Dark current at -0.5 V at different temperatures.

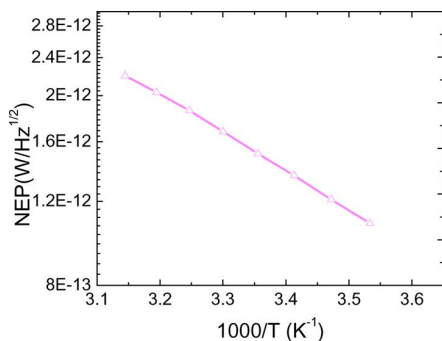


Fig. 7. Johnson noise limited NEP as a function of temperature.

ment results of grating couplers, we can estimate coupling loss at this wavelength to be larger than -9 dB at this wavelength. Therefore, we obtain a minimum peak responsivity of 0.44 A/W corresponding to 24% quantum efficiency. The dark current as a function of temperature is shown in Fig. 6 (at -0.5 V). It decreases significantly as the temperature decreases.

The noise equivalent power (NEP) at 0 V bias as a function of the temperature is calculated [13] and plotted in Fig. 7. It decreases gradually due to the increase of shunt resistance when the temperature decreases.

The Johnson-noise limited NEP is equal to $1.51 \times 10^{-12}\text{ W/Hz}^{1/2}$ obtained at 25°C , corresponding to a responsivity of 0.44 A/W . This represents a Johnson noise limited detectivity D^* of $1.63 \times 10^9\text{ cmHz}^{1/2}/\text{W}$. An R_0A of $0.25\ \Omega \cdot \text{cm}^2$ is obtained on these devices. The overall performance of this device is not as good as the previous reports on standalone nonintegrated devices [3], [14]. This is

due to the smaller size of the current device which experiences more side wall and therefore results in higher leakage current.

This implies that miniaturization comes at a cost of a decreased detectivity, however, as discussed; process optimization can alleviate this performance degradation compared to stand-alone large area devices.

V. CONCLUSION

In summary, we have demonstrated the first GaInAsSb p-i-n photodetector integrated on and coupled to an SOI waveguide circuit. Our design and fabrication process shows mid-infrared integrated photodetectors with high responsivity and very low dark current. This makes it suitable for integrated spectroscopic system.

ACKNOWLEDGMENT

The authors would like to thank S. Verstyuyft and Z. Yu for processing assistance and L. Van Landschoot for SEM images.

REFERENCES

- [1] D. Barat, J. Angellier, A. Vicet, and Y. Rouillard, "Antimonide-based lasers and DFB laser diodes in the $2\text{--}2.7\ \mu\text{m}$ wavelength range," *Appl. Phys. B*, vol. 90, no. 2, pp. 201–204, 2008.
- [2] J. A. Gupta, P. J. Barrios, J. Lapointe, G. C. Aers, and C. Storey, "Single-mode $2.4\ \mu\text{m}$ InGaAsSb/AlGaAsSb distributed feedback lasers for gas sensing," *Appl. Phys. Lett.*, vol. 95, no. 4, p. 041104, 2009.
- [3] H. Shao, A. Torfi, W. Li, D. Moscicka, and W. I. Wang, "High detectivity AlGaAsSb/InGaAsSb photodetectors grown by molecular beam epitaxy with cutoff wavelength up to $2.6\ \mu\text{m}$," *J. Cryst. Growth*, vol. 311, pp. 1893–1896, Mar. 2009.
- [4] L. Liu, G. Roelkens, J. Van Campenhout, J. Brouckaert, D. Van Thourhout, and R. Baets, "III-V/silicon-on-insulator nanophotonic cavities for optical network-on-chip," *J. Nanosci. Nanotechnol.*, vol. 10, pp. 1461–1472, 2010.
- [5] G. Roelkens, L. Liu, D. Liang, R. Jones, A. Fang, B. Koch, and J. Bowers, "III-V/silicon photonics for on-chip and inter-chip optical interconnects," *Laser Photon. Rev.*, vol. 4, no. 6, pp. 751–779, Nov. 2010.
- [6] J. Brouckaert, G. Roelkens, D. Van Thourhout, and R. Baets, "Compact InAlAs/InGaAs metal-semiconductor-metal photodetectors integrated on silicon-on-insulator waveguides," *IEEE Photon. Technol. Lett.*, vol. 19, no. 19, pp. 1484–1486, Oct. 1, 2007.
- [7] S. B. Samavedam, M. T. Currie, T. A. Langdo, and E. A. Fitzgerald, "High-quality germanium photodiodes integrated on silicon substrates using optimized relaxed graded buffers," *Appl. Phys. Lett.*, vol. 73, no. 15, Aug. 1998.
- [8] I. Vurgaftman, J. R. Meyer, and L. R. Ram-Mohan, "Band parameters for III-V compound semiconductors and their alloys," *J. Appl. Phys.*, vol. 89, no. 11, pp. 5816–5862, Jun. 2011.
- [9] C. Lauer, O. Dier, and M. C. Amann, "Low-resistive metal/n⁺-InAsSb/n-GaSb contacts," *Semicond. Sci. Technol.*, vol. 21, pp. 1274–1277, Jul. 2006.
- [10] W. Bogaerts, P. Dumon, D. Taillaert, V. Wiaux, S. Beckx, B. Luysaert, J. Van Campenhout, D. Van Thourhout, and R. Baets, "SOI nanophotonic waveguide structures fabricated with deep UV lithography," *Phot. Nano. Fund. Appl.*, vol. 2, no. 2, pp. 81–86, 2004.
- [11] E. Tournié and A. Trampert, "MBE growth and interface formation of compound semiconductor heterostructures for optoelectronics," *Phys. Stat. Sol. (b)*, vol. 244, no. 8, pp. 2683–2696, 2007.
- [12] G. Roelkens, J. Brouckaert, D. Van Thourhout, R. Baets, R. Notzel, and M. Smit, "Adhesive bonding of InP/InGaAsP dies to processed silicon-on-insulator wafers using DVS-bis-benzocyclobutene," *J. Electrochem. Soc.*, vol. 153, no. 12, pp. G1015–G1019, 2006.
- [13] F. Trager, *Springer Handbook of Lasers and Optics*. New York: Springer, 2007, ch. 9.
- [14] J. P. Prineas, J. Jager, S. Seyedmohamadi, and J. T. Olesberg, "Leakage mechanism and potential performance of molecular-beam epitaxially grown GaInAsSb $2.4\ \mu\text{m}$ photodiode detectors," *J. Appl. Phys.*, vol. 103, no. 104511, 2008.